

# The Fission Time Project Chamber Project

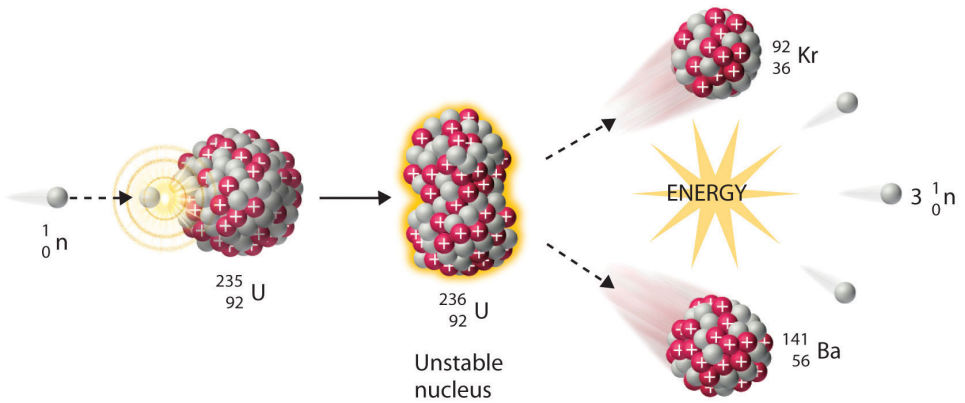
Mike Heffner, Lawrence Livermore National Laboratory  
for the NIFFTE Collaboration

10 Sept 2014

FIESTA 2014

# Improvements in Nuclear Fission Measurements are Still Needed





ChiNu

fission TPC

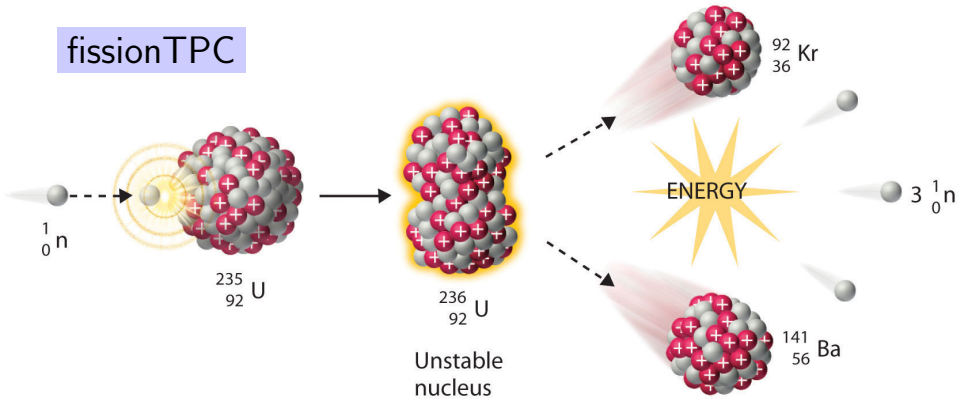
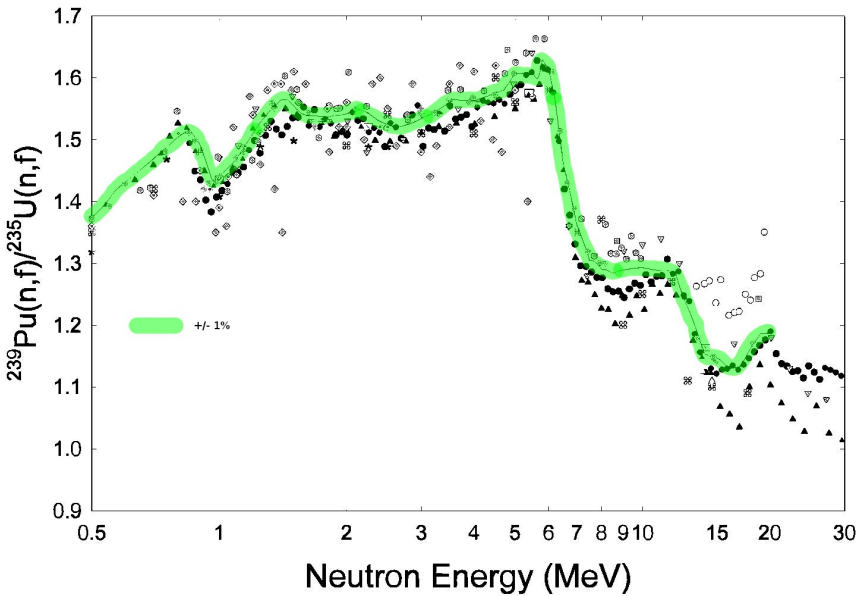


Table 38  
Results of the target accuracy study for the LFR reactor

Isotope	Cross-section	Energy range		Isotope	Cross-section	Energy range		Isotope	Cross-section	Energy range		Uncertainty		
		Initial	Required			Initial	Required			Initial	Required			
U-238	$\sigma_{\text{capt}}$	1.35 MeV–498 keV	5	2.9	Pu-240	$\sigma_{\text{capt}}$	1.35 MeV–498 keV	20	8.4	Zr-90	$\sigma_{\text{el}}$	498–183 keV	20	9.8
		498–183 keV	5	2.4			498–183 keV	20	5.8			183–67.4 keV	20	10.8
		183–67.4 keV	5	2.4			183–67.4 keV	20	5.4			67.4–24.8 keV	20	10.3
		67.4–24.8 keV	5	2.4			67.4–24.8 keV	20	5.7			6.07–2.23 MeV	20	8.6
		24.8–9.12 keV	5	2.7			24.8–9.12 keV	10	6.8	Pb-206	$\sigma_{\text{capt}}$	183–67.4 keV	20	9.8
	$\sigma_{\text{fiss}}$	6.07–2.23 MeV	5	2.6	$\sigma_{\text{fiss}}$	6.07–2.23 MeV	5	4.1		$\sigma_{\text{el}}$	1.35 MeV–498 keV	20	6.3	
		2.23–1.35 MeV	5	2.6			2.23–1.35 MeV	5	3.7			498–183 keV	20	7
	$\sigma_{\text{inel}}$	6.07–2.23 MeV	15	3.8			1.35 MeV–498 keV	5	2.1			19.6–6.07 MeV	40	15.9
		2.23–1.35 MeV	10	3.1			498–183 keV	5	4.1			6.07–2.23 MeV	40	4.6
		1.35 MeV–498 keV	10	2.9	v		1.35 MeV–498 keV	2	1.8			2.23–1.35 MeV	40	4.4
Pu-238	$\sigma_{\text{fiss}}$	498–183 keV	10	4.2	Pu-241	$\sigma_{\text{fiss}}$	1.35 MeV–498 keV	10	4.9			1.35 MeV–498 keV	45	5.3
		183–67.4 keV	10	4.8			498–183 keV	10	3.5	Pb-207	$\sigma_{\text{el}}$	1.35 MeV–498 keV	20	6.8
		1.35 MeV–498 keV	10	4.5			183–67.4 keV	10	3.5			498–183 keV	20	7.5
		498–183 keV	10	4.5			67.4–24.8 keV	10	4.2			19.6–6.07 MeV	40	26.6
		183–67.4 keV	10	6.2			24.8–9.12 keV	10	4.9			6.07–2.23 MeV	40	5.5
		67.4–24.8 keV	30	7.4			9.12–2.03 keV	10	7.3			2.23–1.35 MeV	40	6.7
		24.8–9.12 keV	30	8.7	Pu-242	$\sigma_{\text{fiss}}$	1.35 MeV–498 keV	10	5.3			1.35 MeV–498 keV	45	4
		9.12–2.03 keV	30	12.8	Am-241	$\sigma_{\text{capt}}$	498–183 keV	10	7.3	Pb-208	$\sigma_{\text{el}}$	6.07–2.23 MeV	20	8.4
Pu-239	$\sigma_{\text{capt}}$	498–183 keV	15	5.7			183–67.4 keV	10	7.1			2.23–1.35 MeV	20	7.7
		183–67.4 keV	15	5.4			1.35 MeV–498 keV	10	7.1			1.35 MeV–498 keV	20	3.7
		67.4–24.8 keV	10	6	Am-242m	$\sigma_{\text{fiss}}$	498–183 keV	20	10.9			498–183 keV	20	4.7
		24.8–9.12 keV	10	6.1	Cm-244	$\sigma_{\text{fiss}}$	1.35 MeV–498 keV	40	8.6			19.6–6.07 MeV	40	9.4
	$\sigma_{\text{fiss}}$	6.07–2.23 MeV	5	3.3	Cm-245	$\sigma_{\text{fiss}}$	1.35 MeV–498 keV	40	13.8			6.07–2.23 MeV	40	4.9
		2.23–1.35 MeV	5	2.9			498–183 keV	40	9.6			19.6–6.07 MeV	100	53.1
		1.35 MeV–498 keV	5	1.4			183–67.4 keV	40	10	B-10	$\sigma_{\text{capt}}$	1.35 MeV–498 keV	15	6.1
		498–183 keV	5	1.1			67.4–24.8 keV	40	11.5			498–183 keV	15	3.3
		183–67.4 keV	5	1.2			24.8–9.12 keV	40	14.1			183–67.4 keV	10	3
		67.4–24.8 keV	5	1.5	Fe-56	$\sigma_{\text{el}}$	183–67.4 keV	10	7.1			67.4–24.8 keV	10	3.7
		24.8–9.12 keV	5	1.9		$\sigma_{\text{inel}}$	6.07–2.23 MeV	15	8.5			24.8–9.12 keV	8	4.3
		9.12–2.03 keV	5	3			2.23–1.35 MeV	10	5.6			9.12–2.03 keV	8	6.7
	v	498–183 keV	1	0.9			1.35 MeV–498 keV	20	4.8					

		3.12–2.03 keV	3.12–1.25 keV	1.25–0.5 keV	0.5–0.1 keV	0.1–0.025 keV
Pu-239	$\sigma_{\text{capt}}$	498–183 keV	15	5.7		
		183–67.4 keV	15	5.4		
		67.4–24.8 keV	10	6		
		24.8–9.12 keV	10	6.1		
	$\sigma_{\text{fiss}}$	6.07–2.23 MeV	5	3.3		
		2.23–1.35 MeV	5	2.9		
		1.35 MeV–498 keV	5	1.4		
		498–183 keV	5	1.1		
		183–67.4 keV	5	1.2		
		67.4–24.8 keV	5	1.5		
		24.8–9.12 keV	5	1.9		
		9.12–2.03 keV	5	3		
	$\nu$	498–183 keV	1	0.9		



$$C(E) = w(E) \left[ \epsilon(E) \cdot \Phi(E) + \sum_{i=1}^{N_{\text{isotopes}}} N_i \sigma_i(E) + C^{\text{bkg}}(E) \right]$$

Diagram illustrating the components of the signal count rate  $C(E)$ :

- Detected fission fragments** (red box) feeds into **Live time fraction**.
- Live time fraction** feeds into **Neutron fluence**.
- Neutron fluence** feeds into the sum over isotopes.
- Number of target nuclei** (red box) feeds into the sum over isotopes.
- Background events** (yellow box) feeds into the background term.
- Detection efficiency** (blue box) feeds into the product of fluence and efficiency.
- Sum over isotopes** (green box) feeds into the fission cross section.
- Fission cross section** (orange box) feeds into the final sum term.

$$\frac{\sigma_{P39}}{\sigma_{U35}} = \frac{\epsilon_2}{\epsilon_1} \cdot \frac{N_{U35}}{N_{P39}} \cdot \frac{\Phi_2}{\Phi_1} \cdot \frac{w_1^{-1} \cdot C_1 - C_1^{\text{bkg}}}{w_2^{-1} \cdot C_2 - C_2^{\text{bkg}}} \cdot \text{Background}$$

Relative detection efficiency

Neutron beam distribution

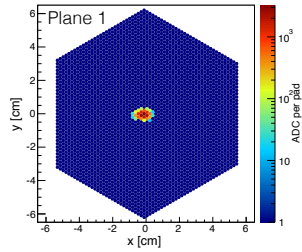
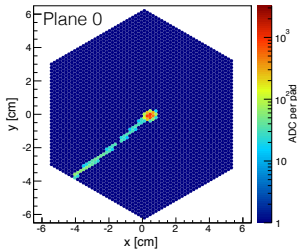
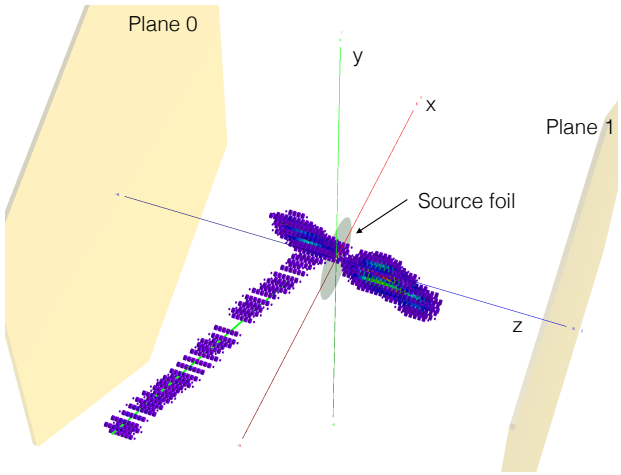
Detector line time

Number of detected FF

Cross section ratio

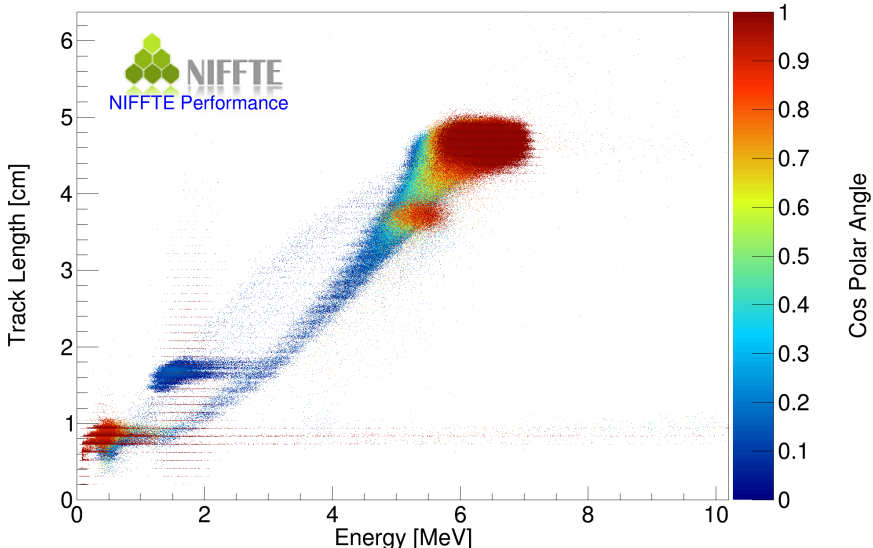
Atom density distribution

Background



$$\frac{\sigma_{P39}}{\sigma_{U35}} = \frac{\epsilon_2}{\epsilon_1} \cdot \frac{N_{U35}}{N_{P39}} \cdot \frac{\phi_2}{\phi_1} \cdot \frac{w_1^{-1} \cdot C_1 - C_1^{\text{bkg}}}{w_2^{-1} \cdot C_2 - C_2^{\text{bkg}}}$$

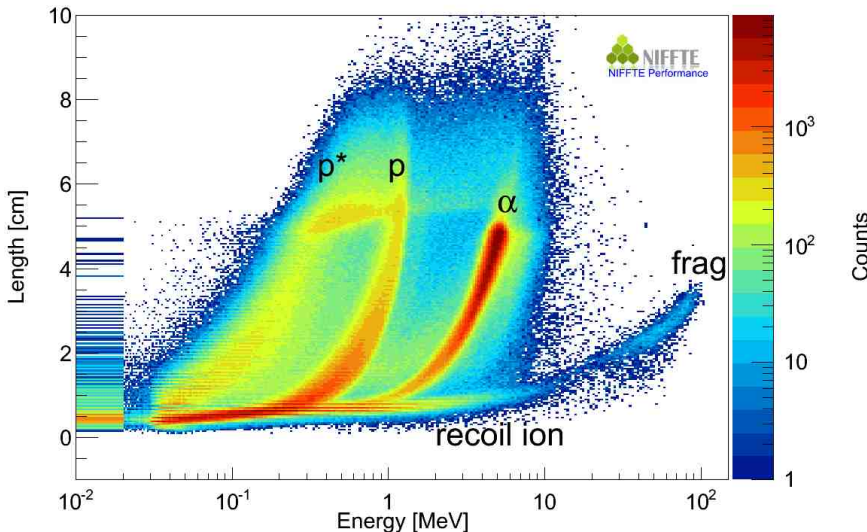
## Track Length vs Energy - Color scale: polar angle



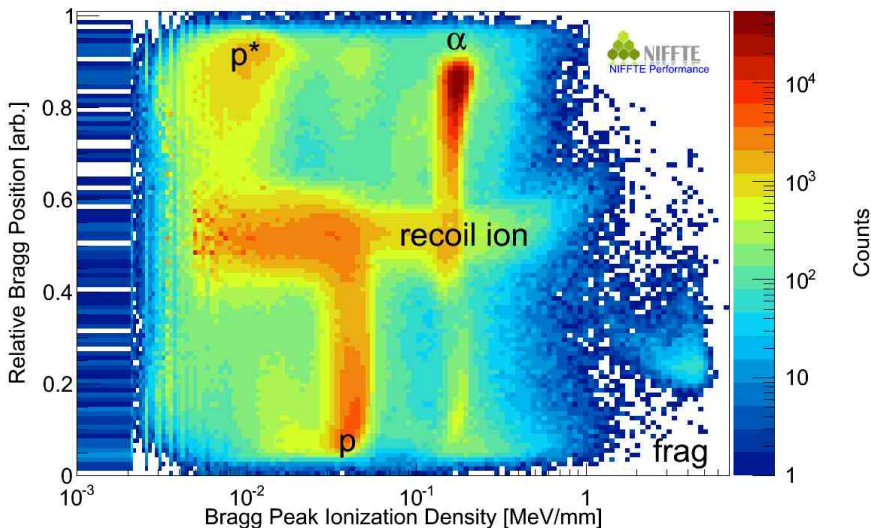


poly

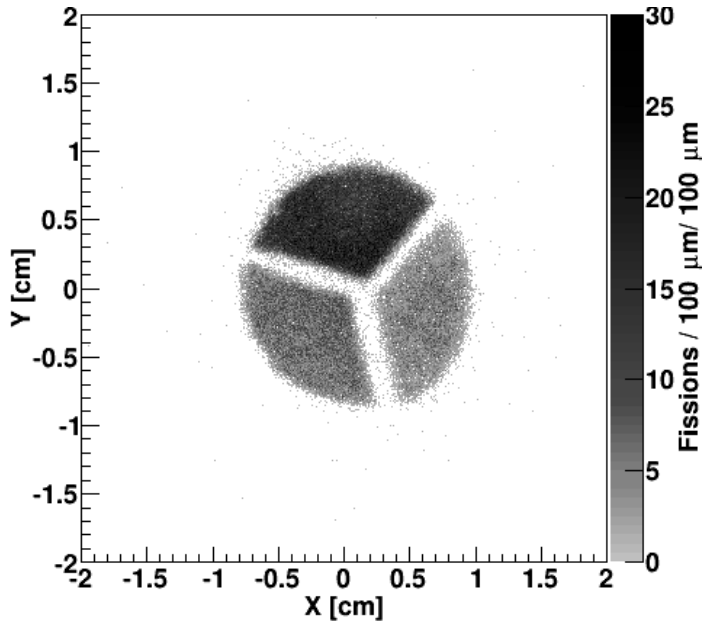
$$\frac{\sigma_{P39}}{\sigma_{U35}} = \left( \frac{\epsilon_2}{\epsilon_1} \right) \cdot \frac{N_{U35}}{N_{P39}} \cdot \frac{\phi_2}{\phi_1} \cdot \frac{w_1^{-1} \cdot C_1 - C_1^{\text{bkg}}}{w_2^{-1} \cdot C_2 - C_2^{\text{bkg}}}$$



$$\frac{\sigma_{P39}}{\sigma_{U35}} = \frac{\epsilon_2}{\epsilon_1} \cdot \frac{N_{U35}}{N_{P39}} \cdot \frac{\phi_2}{\phi_1} \cdot \frac{w_1^{-1} \cdot C_1 - C_1^{\text{bkg}}}{w_2^{-1} \cdot C_2 - C_2^{\text{bkg}}}$$



$$\frac{\sigma_{P39}}{\sigma_{U35}} = \frac{\epsilon_2}{\epsilon_1} \cdot \frac{N_{U35}}{N_{P39}} \cdot \frac{\Phi_2}{\Phi_1} \cdot \frac{w_1^{-1} \cdot C_1 - C_1^{\text{bkg}}}{w_2^{-1} \cdot C_2 - C_2^{\text{bkg}}}$$

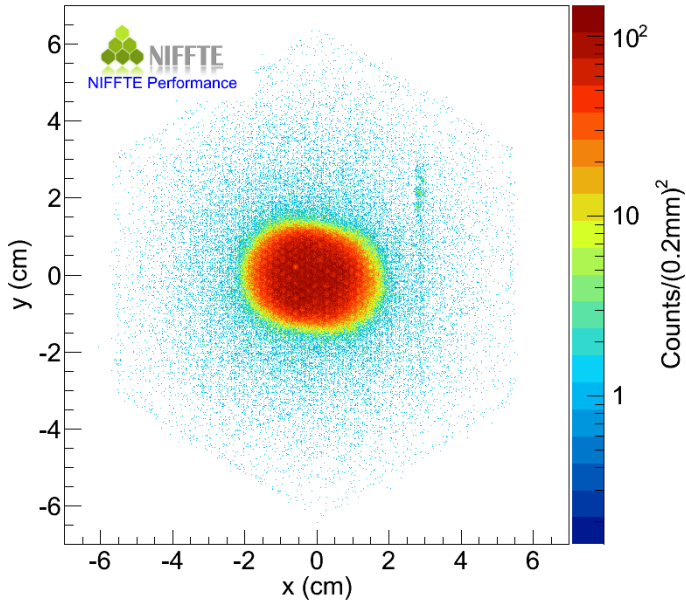


D-3

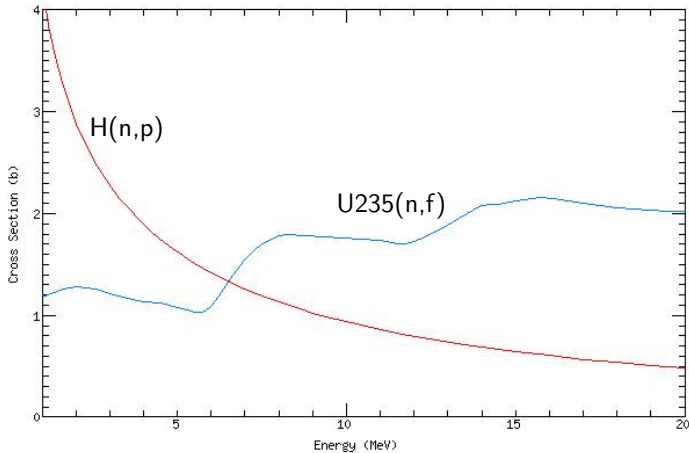
239

522

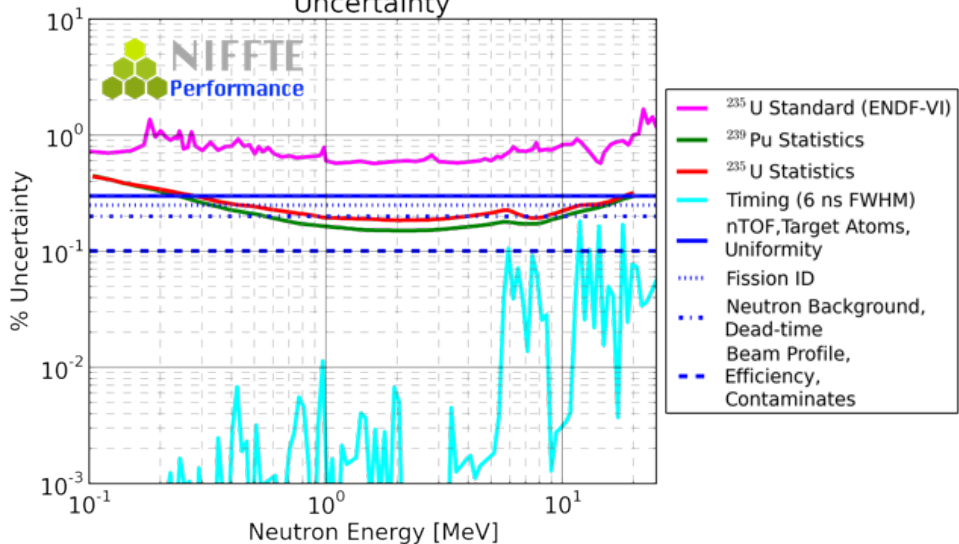
$$\frac{\sigma_{P39}}{\sigma_{U35}} = \frac{\epsilon_2}{\epsilon_1} \cdot \frac{N_{U35}}{N_{P39}} \cdot \frac{\Phi_2}{\Phi_1} \cdot \frac{w_1^{-1} \cdot C_1 - C_1^{\text{bkg}}}{w_2^{-1} \cdot C_2 - C_2^{\text{bkg}}}$$



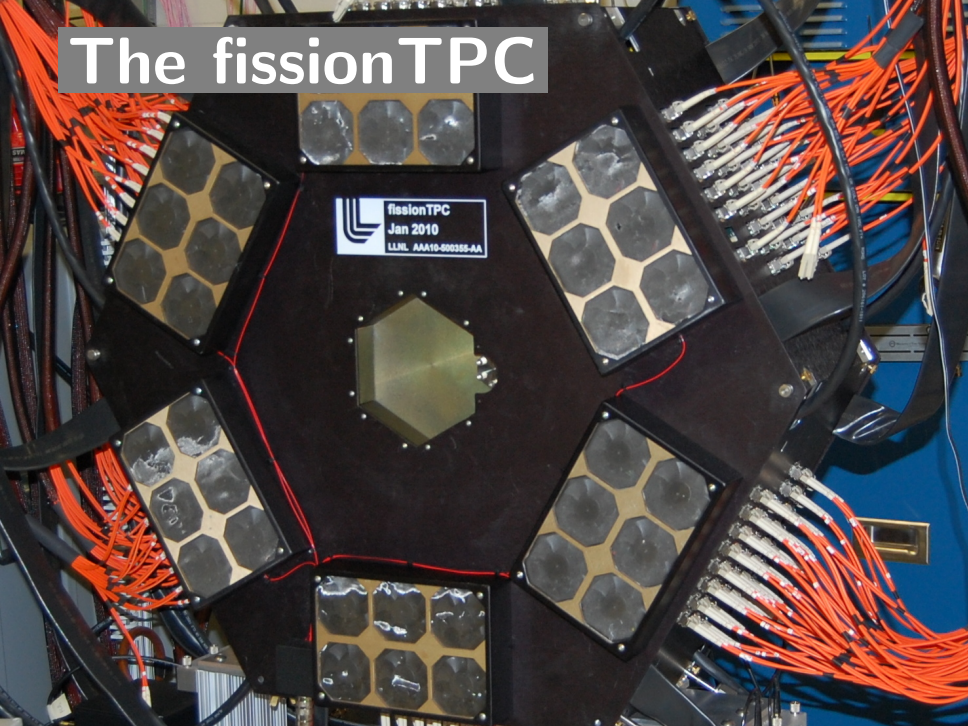
$$\frac{\sigma_{P39}}{\sigma_{U35}} = \frac{\epsilon_2}{\epsilon_1} \cdot \frac{N_{U35}}{N_{P39}} \cdot \frac{\Phi_2}{\Phi_1} \cdot \frac{w_1^{-1} \cdot C_1 - C_1^{\text{bkg}}}{w_2^{-1} \cdot C_2 - C_2^{\text{bkg}}}$$

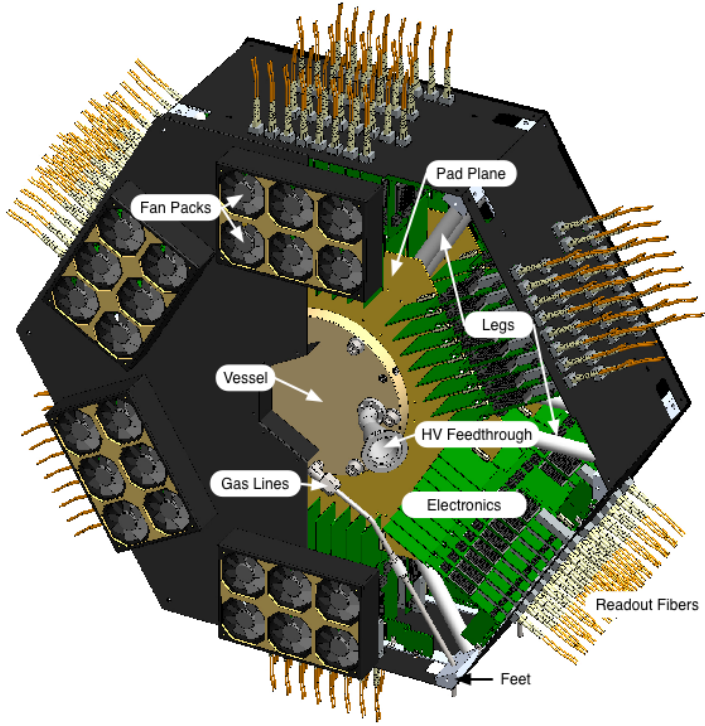


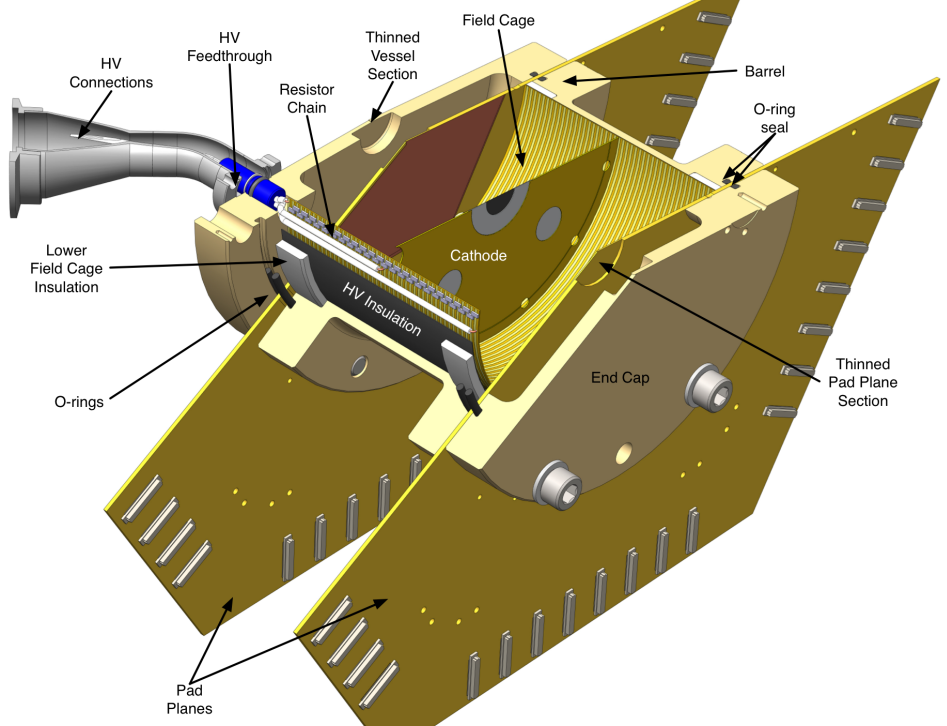
## Expected 2014 Target A Uncertainty



# The fissionTPC







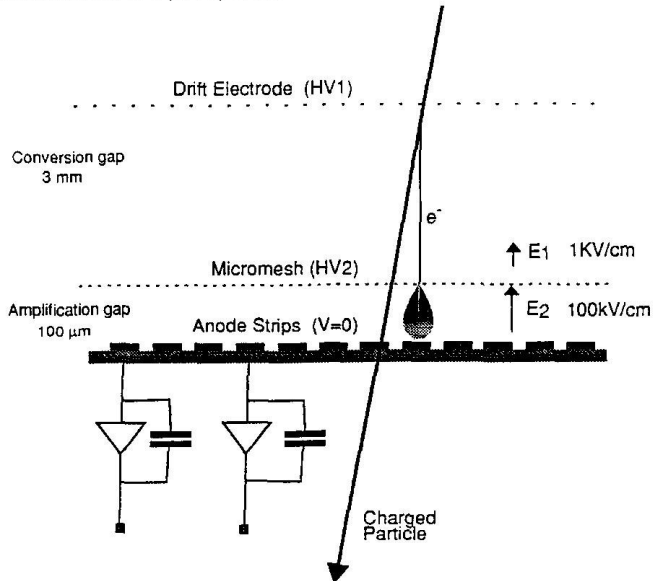
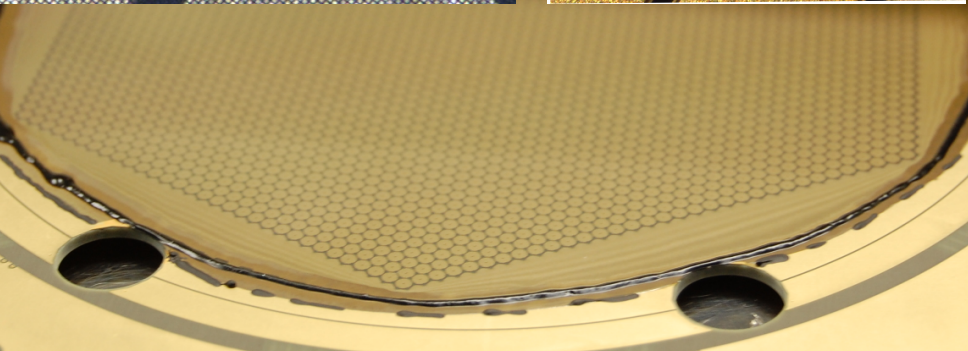
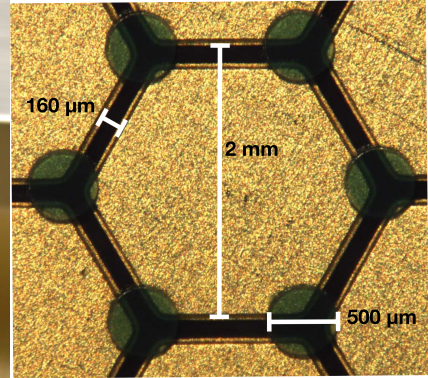
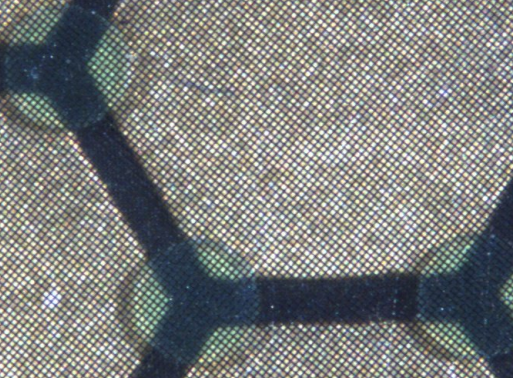
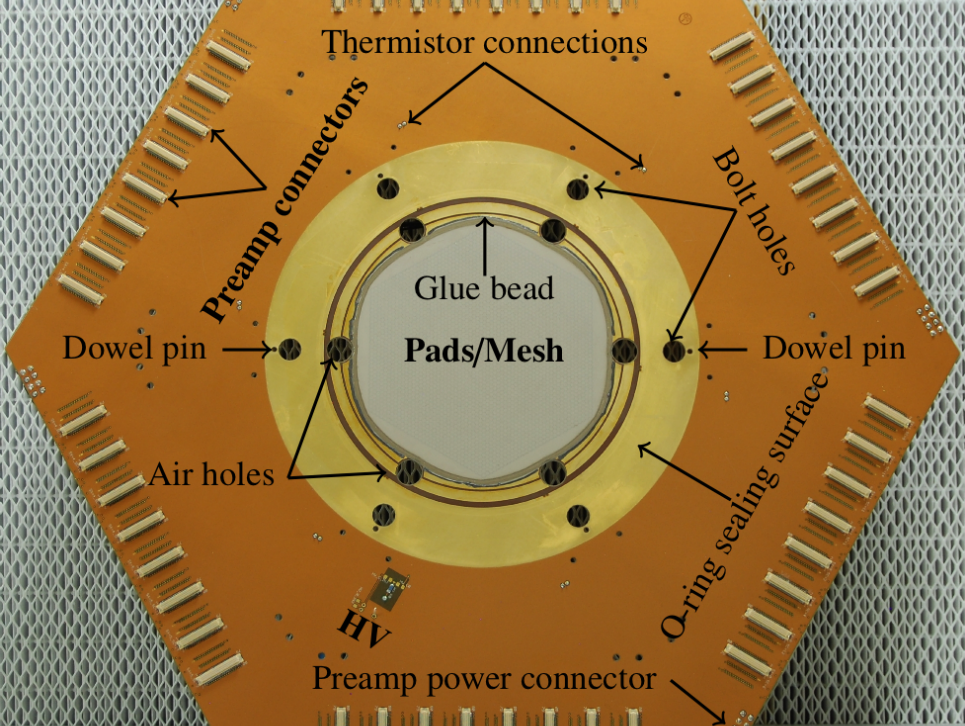
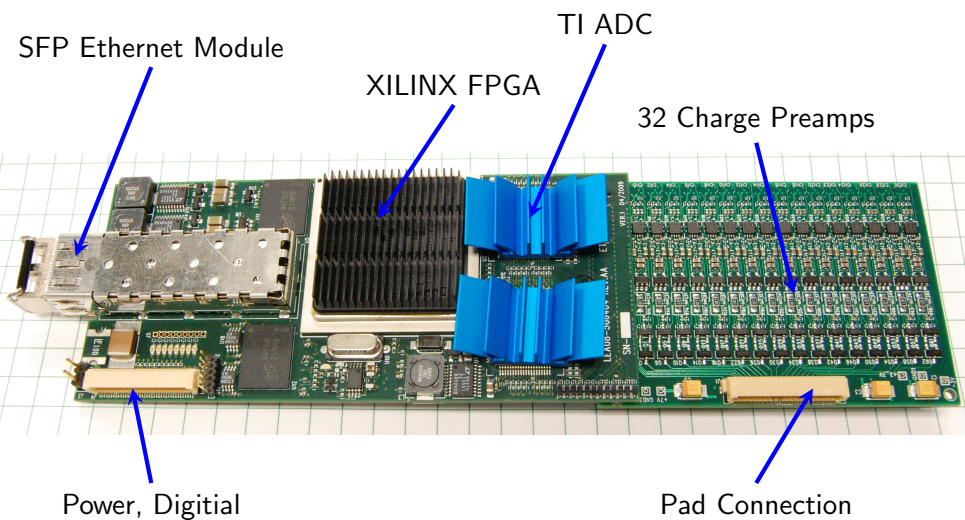
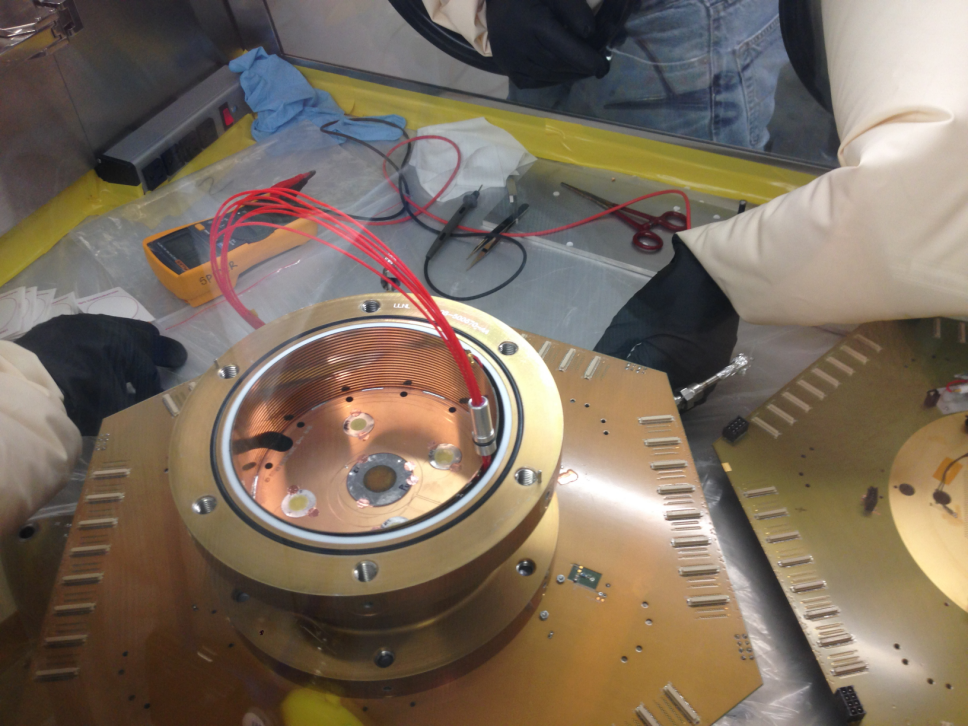


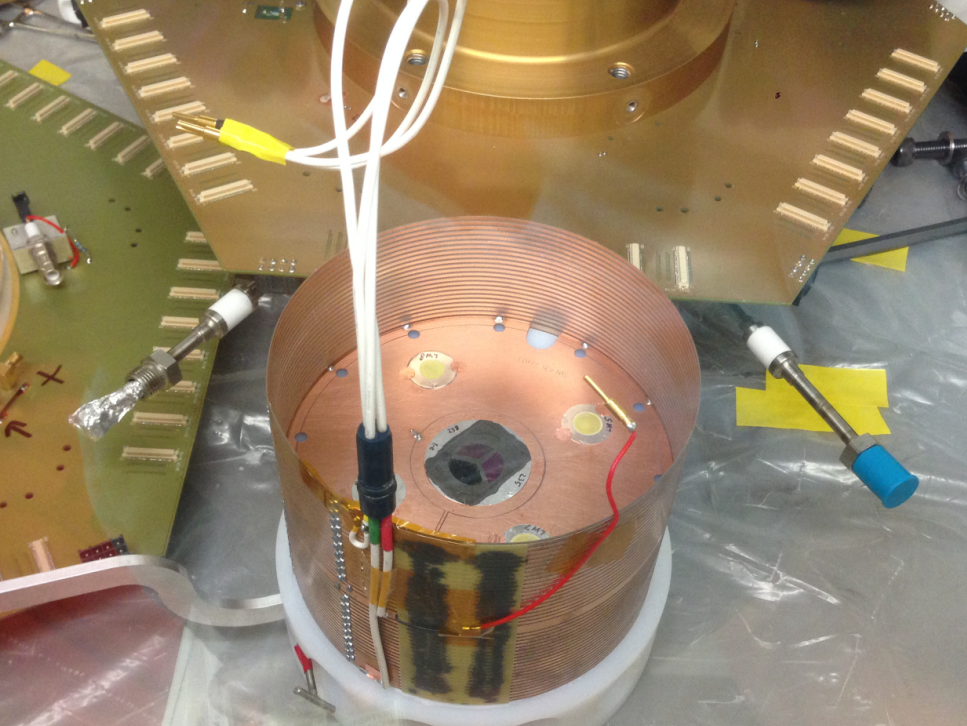
Fig. 1. A schematic view of MICROMEGAS: the 3 mm conversion gap and the amplification gap separated by the micromesh and the anode strip electrode.

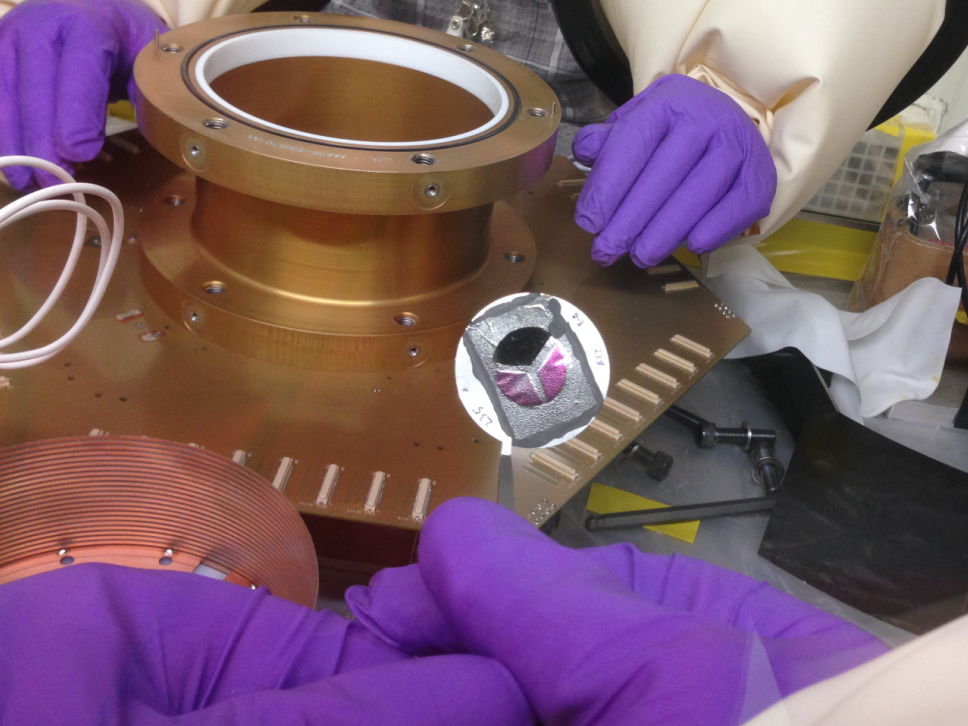














Contents lists available at ScienceDirect

# Nuclear Instruments and Methods in Physics Research A

journal homepage: [www.elsevier.com/locate/nima](http://www.elsevier.com/locate/nima)



## A time projection chamber for high accuracy and precision fission cross-section measurements



M. Heffner <sup>a,\*</sup>, D.M. Asner <sup>b</sup>, R.G. Baker <sup>c</sup>, J. Baker <sup>d,1</sup>, S. Barrett <sup>e</sup>, C. Brune <sup>f</sup>, J. Bundgaard <sup>g</sup>, E. Burgett <sup>h,i</sup>, D. Carter <sup>a</sup>, M. Cunningham <sup>a</sup>, J. Deaven <sup>h</sup>, D.L. Duke <sup>g,k,c</sup>, U. Greife <sup>g</sup>, S. Grimes <sup>f</sup>, U. Hager <sup>g</sup>, N. Hertel <sup>i</sup>, T. Hill <sup>d,k</sup>, D. Isenhower <sup>j</sup>, K. Jewell <sup>d</sup>, J. King <sup>e</sup>, J.L. Klay <sup>c</sup>, V. Kleinrath <sup>h</sup>, N. Kornilov <sup>f</sup>, R. Kudo <sup>c</sup>, A.B. Laptev <sup>k</sup>, M. Leonard <sup>e</sup>, W. Loveland <sup>e</sup>, T.N. Massey <sup>f</sup>, C. McGrath <sup>h</sup>, R. Meharchand <sup>k</sup>, L. Montoya <sup>k</sup>, N. Pickle <sup>j</sup>, H. Qu <sup>j</sup>, V. Riot <sup>a</sup>, J. Ruz <sup>a</sup>, S. Sangiorgio <sup>a</sup>, B. Seilhan <sup>a</sup>, S. Sharma <sup>j</sup>, L. Snyder <sup>a,g</sup>, S. Stave <sup>b</sup>, G. Tatishvili <sup>b</sup>, R.T. Thornton <sup>j</sup>, F. Tovesson <sup>k</sup>, D. Towell <sup>j</sup>, R.S. Towell <sup>j</sup>, S. Watson <sup>j</sup>, B. Wendt <sup>h</sup>, L. Wood <sup>b</sup>, L. Yao <sup>e</sup>

<sup>a</sup> Lawrence Livermore National Laboratory, Livermore, CA 94550, United States

<sup>b</sup> Pacific Northwest National Laboratory, Richland, WA 99354, United States

<sup>c</sup> California Polytechnic State University, San Luis Obispo, CA 93407, United States

<sup>d</sup> Idaho National Laboratory, Idaho Falls, ID 83415, United States

<sup>e</sup> Oregon State University, Corvallis, OR 97331, United States

<sup>f</sup> Ohio University, Athens, OH 45701, United States

<sup>g</sup> Colorado School of Mines, Golden, CO 80401, United States

<sup>h</sup> Idaho State University, Pocatello, ID 83209, United States

<sup>i</sup> Georgia Institute of Technology, Atlanta, GA 30332, United States

<sup>j</sup> Abilene Christian University, Abilene, TX 79699, United States

<sup>k</sup> Los Alamos National Laboratory, Los Alamos, NM 87545, United States

NIFFTE Collaboration

# Conclusions

- Achieving better than 1% total uncertainty for  $^{239}Pu(n, f)$  is difficult and requires analysis of many issues
- The fissionTPC project has shown the potential to illuminate a number of factors simultaneously
- Construction is largely completed; data taking and analysis are now the focus.